Monthly Notices
of the
ROYAL ASTRONOMICAL SOCIETY

MNRASL **431,** L28–L32 (2013) doi:10.1093/mnrasl/slt002
Advance Access publication 2013 February 4

Cross-correlation of *WMAP7* and the *WISE* full data release

András Kovács,[1,2]★ István Szapudi,[3] Benjamin R. Granett[4] and Zsolt Frei[1,2]

[1]*Institute of Physics, Eötvös Loránd University, Pázmány Péter sétány 1/A, H-1117 Budapest, Hungary*
[2]*MTA-ELTE EIRSA 'Lendulet' Astrophysics Research Group*
[3]*Institute for Astronomy, University of Hawaii, 2680 Woodlawn Drive, Honolulu, HI 96822, USA*
[4]*Istituto Nazionale di Astrofisica - Osservatorio Astronomico di Brera, Via E. Bianchi 46, I-23807 Merate, Italy*

Accepted 2013 January 2. Received 2012 December 21; in original form 2012 October 28

ABSTRACT

We measured the cross-correlation of the *Wilkinson Microwave Anisotropy Probe* (*WMAP*) 7-year temperature map and the full sky data release of the *Wide-field Infrared Survey Explorer* galaxy map. Using careful map-making and masking techniques we find a positive cross-correlation signal. The results are fully consistent with a ΛCDM universe, although not statistically significant. Our findings are robust against changing the Galactic latitude cut from $|b| > 10^\circ$ to $|b| > 20^\circ$ and no colour dependence was detected when we used *WMAP Q*, *V* or *W* maps. We confirm higher significance correlations found in the preliminary data release. The change in significance is consistent with cosmic variance.

Key words: dark energy – infrared: galaxies – cosmic background radiation – cosmology: observations – large-scale structure of Universe.

1 INTRODUCTION

Cosmological supernova measurements and cosmic microwave background (CMB) fluctuations support cosmological models in which the cosmic energy density is dominated by dark energy (DE) at the present epoch (Riess et al. 1998; Jarosik et al. 2011). In such theories, the current accelerating expansion and the decay of gravitational potentials are predicted. Therefore, the presence of DE is manifested in both geometrical and dynamical forms.

DE comes to dominate the energy density at late times, $z < 2$, and so the primordial fluctuations in the CMB alone do not provide a sensitive probe. However, DE may leave a signal in the secondary anisotropies that are imprinted on the microwave background radiation. The Integrated Sachs–Wolfe (ISW) effect (Sachs & Wolfe 1967; Rees & Sciama 1968) is an example of a secondary anisotropy: CMB photons passing through a changing gravitational potential become slightly hotter or colder. In a flat and matter-dominated universe, the potential is constant on large scales; thus, gravitational blueshifts and redshifts cancel along the photon path. However, in a universe dominated by DE there is a net energy difference between entering and leaving a potential well due to the decay. Thus, the detection of the linear ISW effect provides direct evidence for DE in the ΛCDM model. Furthermore, alternative gravity models provide predictions for the ISW effect and may be directly tested with ISW observations (Giannantonio et al. 2010).

The ISW signal may be detected through cross-correlation of large-scale structure surveys with the CMB temperature maps. The correlation is weak; generally, less than a 1 μK signal is expected, orders of magnitude below the primary fluctuations. Furthermore, the ISW effect is strongest on large angular scales where cosmic variance is also large, making the measurement even more cumbersome.

Several measurements have been performed to uncover the ISW signal: positive cross-correlations were measured using galaxy data from the Sloan Digital Sky Survey (SDSS) and *Wilkinson Microwave Anisotropy Probe* (*WMAP*; Jarosik et al. 2011) (Fosalba, Gaztañaga & Castander 2003; Padmanabhan et al. 2005; Granett, Neyrinck & Szapudi 2008, 2009; Pápai, Szapudi & Granett 2011). Other successful attempts were Fosalba & Gaztañaga (2004) based on APM galaxies, Nolta et al. (2004) and Raccanelli et al. (2008) using radio data, and Boughn & Crittenden (2004a,b) in which the hard X-ray background was investigated. Besides, Afshordi, Loh & Strauss (2004), Rassat et al. (2007) and Francis & Peacock (2010) used infrared galaxy samples to characterize the ISW signal. The typical ISW significance in the papers above is around 2–3σ. Comprehensive studies using combinations of data sets were carried out by Ho et al. (2008) and Giannantonio et al. (2008, 2012).

The *Wide-field Infrared Survey Explorer* (*WISE*; Wright et al. 2010) all-sky survey is an attractive data set for ISW studies. The survey effectively probes low redshift, $z < 0.3$, with a high source density. Using the preliminary data release (PDR) covering 10 000 deg^2, Goto, Szapudi & Granett (2012) cross-correlated a *WISE* galaxy sample with the CMB, finding a 3σ detection, although with three times the amplitude expected in ΛCDM. In this paper, we re-examine this finding using the full-sky data release (FDR) of the *WISE* survey and the *WMAP* 7-year data set.

The structure of this paper is as follows. In Section 2, we describe the data we used in particular. Section 3 describes our methods including the theoretical expectations, simulations and measurements. Finally, in Section 4 the statistical significances are presented and systematic effects are discussed.

★ E-mail: andraspankasz@gmail.com

2 CMB DATA AND GALAXY MAP

We used the best achievable versions of the CMB data products and focused on the reliability of our new galaxy sample. In this section, we describe our map-making and masking procedures.

2.1 CMB map

The 7-year *WMAP* temperature data were downloaded from the LAMBDA website [1] (Jarosik et al. 2011). *WMAP* data are affected by noise and contaminations both from point sources and from the Milky Way. Among all, the *Q*, *V* and *W* maps have the least Galactic contamination. We used the foreground-reduced version of these maps and the CMB extended temperature mask was chosen to avoid contaminations.

Using HEALPix (Górski et al. 2005), NSIDE = 128 repixelized versions of the maps were created. Galactic foregrounds and known point sources are quite surely excluded and 71 per cent of the sky is unmasked.

2.2 *WISE* galaxy map

The density map of the galaxies was prepared using the FDR of the *WISE* project (Wright et al. 2010). The *WISE* satellite surveyed the sky at four different wavelengths: 3.4, 4.6, 12 and 22 μm. We used different bands to separate stars from galaxies using colour–colour plots. Following Goto et al. (2012) we select sources to a flux limit of W1 $\leq$ 15.2 mag to have a uniform data set.

According to Goto et al. (2012) the majority of stars near to the Galactic plane have a $W_{3.4} - W_{4.6} \leq 0.2$ mag colour. Moreover, it was found that a $W_{4.6} - W_{12} \leq 2.9$ mag selection reduced the stellar contamination. We confirm these findings in the FDR and followed the same procedure for star–galaxy separation.

Our galaxy sample exhibits stripe-like overdensities on the map in several locations, as shown in Fig. 1. While Goto et al. (2012) applied handmade cutouts in their mask to exclude regions with unusually high number counts, we understand that the stripe-like features originated from the observational strategy of *WISE* and the position of the moon. We realized that the moon-contamination flag may be used to properly mask these regions. We forced out pixels in which the 'moonlev' flag is higher than 3 in at least one of the bands. This means that the fraction of the used image frames suffered by moon contamination is higher than 30 per cent. Masking regions based upon the moon contamination flag effectively removes the stripe pattern. We cannot address any further residual effects of the moon contamination outside our mask area. We have found that with a more conservative magnitude limit of *W1* < 14.9 overdensities along stripes are reduced in width but do not disappear.

Sources in *WISE* may also be contaminated by artefacts including the haloes of bright stars, ghost images and diffraction spikes, and special data quality flags exist to handle these problems. If the data set is filtered using these flags, we possibly lose real galaxies. However, if we do not use flags to create a conservative catalogue, then stars or galaxies with insufficient parameters can appear in the data. Goto et al. (2012) used additional pixels in their mask to exclude regions where the abundance of these unreliable objects is high, but did not filter the whole galaxy sample. We investigated both cases and we have found this choice is important especially on large scales.

[1] http://lambda.gsfc.nasa.gov/

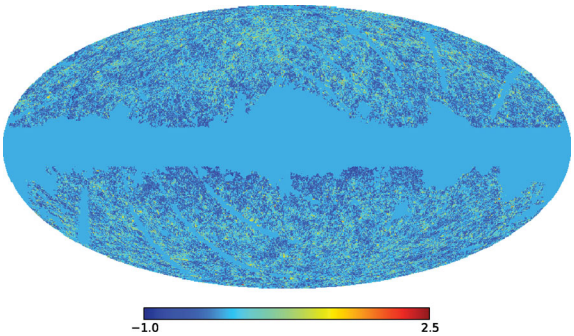

Figure 1. *WISE* all-sky galaxy sample, together with our mask including the stripes and *WMAP*'s mask area.

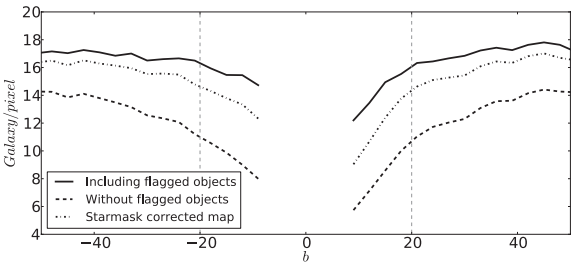

Figure 2. Gradients in galaxy density can be detected as a function of Galactic latitude *b*. The effect is less significant if objects with warning flags are included in the sample, since the density drop is ≈4 per cent at $|b| = 20^\circ$ compared to its value at $|b| = 50^\circ$.

We find a gradient in the galaxy density with Galactic latitude with fewer galaxies near the Galactic plane. An empirical correction was developed by Goto et al. (2012) in which a mean correction is computed in Galactic latitude bins to artificially 'flatten' the distribution at $|b| < 20^\circ$.

We attribute the gradient to stars near the Galactic plane masking background galaxies. The problem is made more severe due to the broad point spread function of *WISE* (6–12 arcsec). We use the Tycho2 star catalogue which reaches a depth of $V < 13$ mag (Høg et al. 2000) to measure the survey area lost around each star. We calibrated a mean relation between *V* magnitude and star halo radius *R* for *WISE*, $R = 9.52 - 0.74V$, with *R* in arcminutes. Any detected sources within this radius of a Tycho star are removed. We then construct a map of the lost area by summing the area attributed to stars in each HEALPix pixel. This map is then used to normalize the galaxy counts. Fig. 2 shows the result of this correction.

Apparently, the density gradient does not disappear, so only a modest correction is possible with our method. Interestingly, we find that the gradient is higher when flagged sources are not included in the sample. The exact source of the gradient is unexplored, but we show that this effect did not mess up our measurements; our findings are robust.

As described, regions nearby the plane of the Milky Way are potentially contaminated, and we consider the most appropriate solution to use $|b| > 20^\circ$ regions. To perform tests with only the preliminary sky coverage area, a mask was created using the area covered by the preliminary survey.

2.3 Redshift distribution

In order to calculate a theoretical ISW expectation, redshift information is needed. Since *WISE* is a photometric survey without

spectroscopy, the selected galaxies were cross-identified with sources from the Galaxy and Mass Assembly (GAMA, Driver et al. 2011) sample that has spectroscopic redshift of ∼200 000 galaxies. Using the overlapping part of the two surveys, we have found a pair for 82 per cent of the galaxies with a 3 arcsec matching radius. We estimated an accidental matching rate of 0.1 per cent for this analysis using random points with *WISE* density. The matched sample has a median redshift $\bar{z} \approx 0.15$. The obtained approximate redshift distribution provides a basis to calculate a theoretical cross-power spectrum in this redshift range.

3 RESULTS

In this section, we discuss the results using the CMB and galaxy data sets. We also elaborate on the most important theoretical and simulated considerations related to ISW detection and further analysis.

3.1 *WISE–WMAP* cross-correlation

We calculate the cross-power spectrum using a fast quadratic estimator SpICE (Spatially Inhomogenous Correlation Estimator, Szapudi et al. 2001, 2005; Szapudi, Prunet & Colombi 2001). The individual band powers are binned logarithmically, the boundaries are $l = 6$, 8, 11, 16, 22, 31, 44, 61 and 87 which means the first band stands for $l = 6$, 7, etc. With this choice we avoid the lowest l range, where cosmic variance is meaningful and it is easier to compare the results to Goto et al. (2012), who used the same bins. Our measurement is introduced in Fig. 3.

3.2 Theory

We derive the expected correlations and galaxy bias using *WMAP7* best-fitting ΛCDM cosmological parameters (Jarosik et al. 2011). Following Francis & Peacock (2010) a linear bias relation is considered to couple galaxy and matter overdensities, $\delta_{\rm g} = b\delta_{\rm m}$. The two-dimensional projection of the 3D galaxy auto-correlation is given by

$$C_{\rm gg}(l) = b_{\rm g}^2 \frac{2}{\pi} \int {\rm d}k\, k^2\, P(k) \left| \int {\rm d}r\, r^2\, \phi(r)\, j_l(kr) \right|^2 , \qquad (1)$$

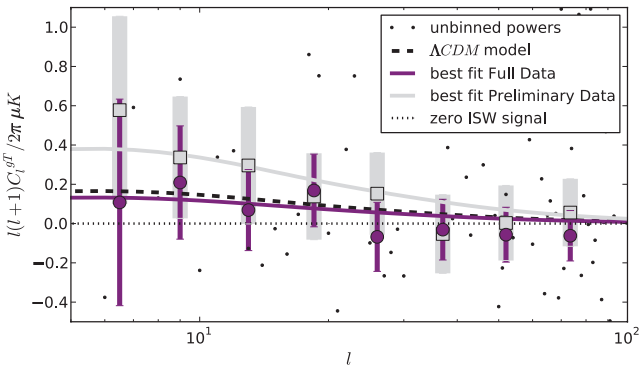

Figure 3. Cross-correlation power spectra of *WMAP7–WISE* data sets using our $|b| > 20^\circ$ mask, together with theoretical expectations for ΛCDM cosmology and zero ISW detection. The magenta error bars were computed using 1000 simulations and the diagonal elements of the covariance matrix. The light-grey error bars represent the variance of the $C_l^{\rm FDR} - C_l^{\rm PDR}$ differences in each bin to check if the change is consistent with cosmic variance.

where $\phi(r) \propto \frac{{\rm d}N(r)}{{\rm d}z} \frac{{\rm d}z}{{\rm d}V}$ is a comoving coordinate with a normalization relation $\int \phi(r) r^2 {\rm d}r = 1$, and j_l is a spherical Bessel function. Independent determination of $b_{\rm g}$ is not possible in linear theory, because σ_8 acts to renormalize the power spectrum, $C_l \propto (b\sigma_8)^2$. Thus, we fit only for $b_{\rm g}$ and keep σ_8 fixed. CosmoPy[2] and CAMB[3] were used to generate non-linear matter power spectra with HALOFIT (Smith et al. 2003) at the median redshift of our galaxy sample.

We measure the galaxy–galaxy power spectrum with SpICE. The measurement is affected by Poissonian shot noise that has a form of $1/N$, where N is the mean galaxy count per steradian. Actually, the impact is negligible, less than 10 per cent at the maximum l we used and less significant at larger scales where we expect to measure the ISW effect. However, to be precise we subtracted the noise, and the amplitude of the theoretical model curve was fitted in the $6 < l < 100$ interval, i.e. angular scales down to ∼2°. Our result is $b_{\rm g} = b\sigma_8 = 1.04 \pm 0.05$.

To bring the $b_{\rm g}$ parameter into use, consider now the expression of the theoretical ISW signal. The cross-spectrum of a galaxy map and the CMB is given by

$$C_l^{{\rm g}T} = b_{\rm g} \frac{6\, T_{\rm CMB} \Omega_{\rm m} {H_0}^2}{\pi c^2} \int {\rm d}k\, k^2\, P_k \times \int {\rm d}r\, j_l(kr) k^{-2} \frac{{\rm d}(1+z) D_1(z)}{{\rm d}r} \int {\rm d}r'\, j_l(kr')\, \phi(r') r'^2 , \qquad (2)$$

where $D_1(z)$ is the linear growth factor; the numerical result of this expression depends on the cosmology (Cooray 2002).

3.3 Simulations

We simulated 1000 random CMB skies with ΛCDM cosmological parameters using HEALPix SYNFAST to cross-correlate with our *WISE* galaxy density map. The power spectrum was calculated and binned into the eight spectral bins given above. The covariance matrix estimated from these measurements is shown in Fig. 4. Neighbouring bins are anti-correlated typically by 10 per cent. The diagonal elements were used to calculate the error bars shown in Fig. 3.

4 SIGNIFICANCE TESTS

Again we follow Francis & Peacock (2010), now to determine the significance of our ISW detection. Consistency of our results was investigated with three hypotheses: null detection of the ISW effect, regular ΛCDM model predictions, and finally with a best-fitting theoretical curve. Our statistics are based on the amplitude fit; we set the amplitude of the ΛCDM theoretical curve to 1.0 and to 0.0 in the zero-ISW case.

4.1 Statistical tools

We evaluate a χ^2 statistic for each hypothesis which is as follows:

$$\chi^2 = \sum_{ij} d_i C_{ij}^{-1} d_j , \qquad (3)$$

where C is the covariance matrix and $d_i = (C_{\rm data}^{{\rm g}T} - C_{\rm hypo}^{{\rm g}T})$. $C_{\rm hypo}^{{\rm g}T}$ can be given by equation (2) assuming various models or it is zero

[2] http://www.ifa.hawaii.edu/cosmopy/
[3] http://camb.info/

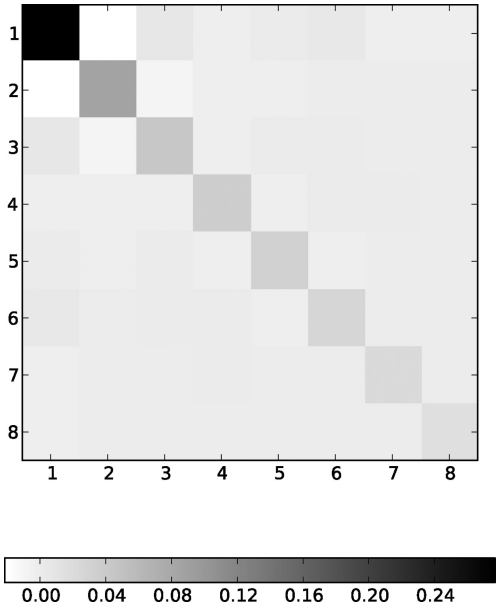

Figure 4. Covariance matrix of the logarithmic spectral bins from 1000 random CMB simulations. Neighbouring bands are not correlated in a good approximation.

in the null-ISW case. Index i labels the bins we use in the cross-spectrum. Moving forward one step, we define the likelihood of a hypothesis below:

$$\mathcal{L} \propto |\mathbf{C}|^{-N/2} \mathrm{e}^{-\frac{1}{2}\boldsymbol{d}^{\mathrm{T}}C^{-1}\boldsymbol{d}}, \quad (4)$$

where N is the number of data points with the vector $\boldsymbol{d}$ constructed using d_i and the $\mathbf{C}$ matrix.

In fact, our tool to describe the detailed statistical properties of our test is $-2\ln(\mathcal{L}_1/\mathcal{L}_2) = \Delta\chi^2$ where the ratio of the two likelihoods is taken in a case of two different hypotheses and $\Delta\chi^2$ is calculated. In general, $\Delta\chi^2 > 3$ is strong evidence for a significant difference.

4.2 Systematic effects

Although we have taken care in source selection and masking, we must address any residual systematic effects that may exist. Galactic dust or emission detected by *WMAP* could contribute to a correlation with *WISE* due to dust attenuation or the gradient in source density measured with the Galactic latitude. However, we performed all the significance tests using Q, V and W foreground reduced CMB maps and the maximum relative difference in a given spectral bin was 1.2 per cent. This fact led us to the conclusion that there is no significant colour dependence and effects from Galactic dust or emission must be minor. We also checked the results using the WMAP team's temperature mask or extended temperature mask but no meaningful difference was found.

On the other hand, we investigated several systematic effects related to our galaxy sample. First, we analysed different Galactic latitude cuts (Table 1). Our finding is robust, even if not significant; the results are summarized in Table 2.

Next we considered the differences in the detection significance due to initial map making. Our tests were applied to a map without flagged objects and it was obtained that the amplitude varies between 0.5 and 1.0 regardless of the star mask correction technique.

We repeated our analysis with the $W1 \leq 14.9$ mag limit to test the effects of faint sources. With this sample originating from a slightly different redshift distribution, we found an increment in the ISW signal, but the error bars were also high so the significance remained $\sim 1.0\sigma$.

We also extended our cross-correlation analysis to $2 \leq l \leq 5$ multipoles and very weak positive cross-correlation was measured with extremely high error bars. The results increased the significance only slightly; however, they were sensitive to the Galactic cut.

In light of the robustness of our results against different Galactic cuts, we argue that the stellar contamination is low or at least uniform in our galaxy sample and it does not affect the measurements. The upper limit is 18 per cent from the *WISE*–GAMA matching but a similar deficit of optical pairs was also reported using SDSS and *WISE* (Yan et al. 2012). These facts all indicate that the different selection criteria of the infrared and the optical bands are responsible for the missing counterparts, rather than confusion with stars. In summary, the presence of stars is probably less than the unpaired fraction of our galaxy sample.

Table 1. Mask properties of the *WISE* galaxy sample. The first three rows correspond to all-sky data with b Galactic latitude cuts. The last mask was made using only the preliminary survey area and an additional $|b| > 10^\circ$ cut.

Mask	Area (deg^2)	$N_{\mathrm{gal}}^{\mathrm{no\ flag}}$	$N_{\mathrm{gal}}^{\mathrm{starcorr}}$	N_{gal}
$\lvert b\rvert > 10^\circ$	26 443	1662 995	2016 563	2234 370
$\lvert b\rvert > 15^\circ$	25 248	1617 745	1948 454	2129 013
$\lvert b\rvert > 20^\circ$	23 167	1521 755	1814 156	1945 517
$\lvert b\rvert > 10^\circ$	10 967	782 502	976 209	1057 073

Table 2. Significance properties of our results are shown. χ^2 values in the table are less than theoretically expected; this indicates that the error bars are possibly overestimated. The same was reported by Francis & Peacock and Rassat et al. in their work. We performed Monte Carlo (MC) runs with 1000 and 3000 trials, but the covariance was robust. Moreover, the analytic estimate of the covariances and errors (Cabré et al. 2007) agrees to 5 per cent with the MC outcomes.

Mask	ISW model	χ^2	$\Delta\chi^2$	Amplitude	Signal-to-noise ratio
	Zero	3.07	–	–	–
$\lvert b\rvert > 10^\circ$	Best fit	2.20	0.87	0.8 ± 0.9	0.9
	ΛCDM	2.26	0.81	–	–
	Zero	2.71	–	–	–
$\lvert b\rvert > 15^\circ$	Best fit	2.13	0.58	0.7 ± 0.9	0.9
	ΛCDM	2.27	0.44	–	–
	Zero	2.32	–	–	–
$\lvert b\rvert > 20^\circ$	Best fit	1.63	0.69	0.8 ± 0.8	1.0
	ΛCDM	1.74	0.58	–	–
$\lvert b\rvert > 10^\circ$	Zero	5.64	–	–	–
preliminary	Best fit	2.91	2.73	2.3 ± 1.2	1.9
area only	ΛCDM	3.74	1.90	–	–

5 DISCUSSION AND CONCLUSIONS

Our principal aim was to produce the final ISW measurement using *WISE*; we compared our results with Goto et al. (2012) that used the PDR. We repeated our measurements with the *WISE* preliminary data and largely reproduced the individual C_l^{gT} powers found by Goto et al. (2012), although we measured lower significance, except using alternative binning. We do not expect perfect agreement, given that the analysis was performed from the ground up. With the same bins our best-fitting amplitude for the PDR was 2.5 ± 1.2,

i.e. a 2.1σ detection. The result is consistent with our 1.9σ finding on the preliminary part of the sky but using the new data. Using the full sky we measure an ISW significance of $\sim$1.0σ. The change is fully consistent with possible cosmic variance, as illustrated by the light grey error bars in Fig. 3.

With our enhanced map making and better view of the *WISE* data, we suppressed artefacts. Our mask is entirely based on the properties of the *WISE* object flags and many systematics were revealed. However, the signal decreased despite the improvements in our analysis methods.

While some recent studies, especially Goto et al. (2012), raised the possibility that the ISW correlations might be higher than ΛCDM predictions, we conclude that the signal we found is consistent with ΛCDM and previous measurements (Rassat et al. 2007; Francis & Peacock 2010). Our analysis highlighted that higher ISW amplitude measurements on certain parts of the sky can be due to cosmic variance.

ACKNOWLEDGEMENTS

We take immense pleasure in thanking the support of NASA grants NNX12AF83G and NNX10AD53G and the Polanyi programme of the Hungarian National Office for the Research and Technology (NKTH). BRG acknowledges support from PRIN INAF 2010. In addition, AK and ZF acknowledge support from OTKA through grant no. 101666. We are very thankful to Luigi Guzzo because of his help with the collaborative work of AK and BRG in Merate. Finally, yet importantly, we thank the useful suggestions of the WISE team.

REFERENCES

Afshordi N., Loh Y.-S., Strauss M. A., 2004, Phys. Rev. D, 69, 083524
Boughn S., Crittenden R., 2004a, Nat, 427, 45
Boughn S. P., Crittenden R. G., 2004b, ApJ, 612, L647
Cabré A., Fosalba P., Gaztañaga E., Manera M., 2007, MNRAS, 381, 1347
Cooray A., 2002, Phys. Rev. D, 65, 103510
Driver S. P. et al., 2011, MNRAS, 413, 971
Fosalba P., Gaztañaga E., 2004, MNRAS, 350, L37
Fosalba P., Gaztañaga E., Castander F. J., 2003, ApJ, 597, L89
Francis C. L., Peacock J. A., 2010, MNRAS, 406, 2
Giannantonio T., Scranton R., Crittenden R. G., Nichol R. C., Boughn S. P., Myers A. D., Richards G. T., 2008, Phys. Rev. D, 77, 123520
Giannantonio T., Martinelli M., Silvestri A., Melchiorri A., 2010, J. Cosmol. Astropart. Phys., 4, 30
Giannantonio T., Crittenden R. G., Nichol R. C., Ross A. J., 2012, MNRAS, 426, 2581
Górski K. M., Hivon E., Banday A. J., Wandelt B. D., Hansen F. K., Reinecke M., Bartelman M., 2005, ApJ, 622, 759
Goto T., Szapudi I., Granett B. R., 2012, MNRAS, 422, L77
Granett B. R., Neyrinck M. C., Szapudi I., 2008, ApJ, 683, L99
Granett B. R., Neyrinck M. C., Szapudi I., 2009, ApJ, 701, 414
Ho S., Hirata C., Padmanabhan N., Seljak U., Bahcall N., 2008, Phys. Rev. D, 78, 043519
Høg E. et al., 2000, A&A, 355, L27
Jarosik N. et al., 2011, ApJS, 192, 14
Nolta M. R. et al., 2004, ApJ, 608, L10
Padmanabhan N., Hirata C. M., Seljak U., Schlegel D. J., Brinkmann J., Schneider D. P., 2005, Phys. Rev. D, 72, 043525
Pápai P., Szapudi I., Granett B. R., 2011, ApJ, 732, L27
Raccanelli A., Bonaldi A., Negrello M., Matarrese S., Tormen G., de Zotti G., 2008, MNRAS, 386, 2161
Rassat A., Land K., Lahav O., Abdalla F. B., 2007, MNRAS, 377, 1085
Rees M. J., Sciama D. W., 1968, Nat, 217, 511
Riess A. G. et al., 1998, AJ, 116, 1009
Sachs R. K., Wolfe A. M., 1967, ApJ, 147, L73
Smith R. E. et al., 2003, MNRAS, 341, 1311
Szapudi I. et al., 2001, ApJ, 548, L115
Szapudi I., Prunet S., Colombi S., 2001, ApJ, 561, L11
Szapudi I., Pan J., Prunet S., Budavári T., 2005, ApJ, 631, L1
Wright E. L. et al., 2010, AJ, 140, 1868
Yan L. et al., 2012, ApJ, 145, 16

This paper has been typeset from a TEX/LATEX file prepared by the author.